

# Continuum bound states $K_L$ , $D_1(2420)$ , $D_{s1}(2536)$ , and their partners $K_S$ , $D_1(2400)$ , $D_{sJ}^*(2463)$

Eef van Beveren

*Centro de Física Teórica*

*Departamento de Física, Universidade de Coimbra*

*P-3000 Coimbra, Portugal*

eef@teor.fis.uc.pt

George Rupp

*Centro de Física das Interações Fundamentais*

*Instituto Superior Técnico, Edifício Ciência*

*P-1049-001 Lisboa Codex, Portugal*

george@ajax.ist.utl.pt

PACS number(s): 12.40.Yx, 14.40.Aq, 14.40.Lb, 13.25.Es, 13.25.Ft, 13.75.Lb

May 22, 2019

## Abstract

The very recently observed  $D_{sJ}^*(2463)$  meson is described as a  $J^P = 1^+ c\bar{s}$  bound state in a unitarised meson model, owing its existence to the strong OZI-allowed  $^3P_0$  coupling to the nearby  $S$ -wave  $D^*K$  threshold. By the same non-perturbative mechanism, the narrow axial-vector  $D_{s1}(2536)$  resonance shows up as a quasi-bound-state partner embedded in the  $D^*K$  continuum. With the same model and parameters, it is also shown that the preliminary broad  $1^+ D_1(2400)$  resonance and the established narrow  $1^+ D_1(2420)$  may be similar partners, as a result of the strong OZI-allowed  $^3P_0$  coupling to the nearby  $S$ -wave  $D^*\pi$  threshold. The employed mechanism also reproduces the  $K_L$ - $K_S$  mass difference and the  $K_S$  width, by describing  $K_L$  as a bound state embedded in the  $\pi\pi$  continuum.

The continuum bound states  $D_1(2420)$  and  $D_{s1}(2536)$  are found to be mixtures of 33%  $^3P_1$  and 67%  $^1P_1 c\bar{n}$ , respectively  $c\bar{s}$ . Whereas their partners  $D_1(2400)$  and  $D_{sJ}^*(2463)$  are found to have more or less the opposite content, but additionally with some  $D^*\pi$ , respectively  $D^*K$  admixture.

## 1 Introduction

Bound states embedded in the continuum have been suggested by von Neumann and Wigner [1]. Since then many works on this theme have appeared in various fields of physics [2–6]. In the

present paper, we shall study such states appearing as (approximate) solutions of our simple unitarised meson model [7]. As three concrete applications, we choose here the  $K_L$ - $K_S$  system, the  $D_{s1}(2536)$  [8] together with the very recently observed narrow  $D_{sJ}^*(2463)$  [9] state, and finally the couple consisting of the established  $D_1(2420)$  [8] and the preliminary broad  $D_1(2400)$  [10,11] resonance. At first sight, it may seem odd to try to relate such utterly disparate states, ranging from mesons that can only decay weakly to very broad mesonic resonances. Moreover, while in the  $J^P = 1^+ c\bar{n}$  ( $n$  stands for non-strange) system the  $D_1(2400)$  is much broader than the slightly heavier  $D_1(2420)$ , for the  $c\bar{s}$  states the likely  $1^+ D_{sJ}^*(2463)$  is *even narrower* than the  $1^+ D_{s1}(2536)$ . Nevertheless, we shall demonstrate below that, in all three cases, a simple mechanism of coupling two degenerate  $q\bar{q}$  channels with the same quantum numbers to the meson-meson continuum is capable of accounting for the experimental data, through an exact or approximate decoupling of one of the physical  $q\bar{q}$  states.

## 2 Degeneracy lifting via coupling to the continuum

When two degenerate discrete channels are coupled to the same continuum channel, the degeneracy is lifted. One state decouples, partly or completely, depending on the details of the interaction dynamics, and turns into a continuum (approximate) bound state. The other state turns into either a resonance structure in the continuum, or a bound state below threshold when threshold is near enough. Within our unitarisation scheme, quark-antiquark channels are coupled to the meson-meson continuum by OZI-allowed  $^3P_0$   $q\bar{q}$  pair creation and annihilation.

In the present investigation, we confine our attention to two degenerate quark-antiquark systems, which can be distinguished by some internal structure irrelevant for the coupling to the meson-meson continuum. Let us denote by  $\psi_1$  and  $\psi_2$  the wave functions of the quark-antiquark systems, and by  $H_1$  and  $H_2$  the Hamiltonians describing their internal confinement dynamics. For the continuum we write the wave function  $\psi$  and the dynamics  $H$ . The coupling interactions of the two confinement channels to the continuum are denoted by  $V_1$  and  $V_2$ . In the spirit of our model, we then obtain for the three channels the set of coupled dynamical equations

$$\begin{aligned} (H - E) \psi + V_1 \psi_1 + V_2 \psi_2 &= 0 \\ V_1^\dagger \psi + (H_1 - E) \psi_1 &= 0 \\ V_2^\dagger \psi + (H_2 - E) \psi_2 &= 0 \end{aligned} \quad . \tag{1}$$

We assume that the internal dynamics of the two degenerate quark-antiquark systems does not depend on the difference in their internal structure, and, moreover, that these systems also couple

the same way to the continuum, i.e.,

$$H_1 = H_2 \quad \text{and} \quad V_1 = \alpha V \quad , \quad V_2 = \beta V \quad (\alpha^2 + \beta^2 = 1) . \quad (2)$$

In this case it is easy to sub-diagonalise the system (1), so as to obtain

$$\begin{aligned} (H - E) \psi + V (\alpha\psi_1 + \beta\psi_2) &= 0 \\ V^\dagger \psi + (H_1 - E) (\alpha\psi_1 + \beta\psi_2) &= 0 \end{aligned} \quad (3)$$

and

$$(H_1 - E) (\beta\psi_1 - \alpha\psi_2) = 0 . \quad (4)$$

We end up with a system of the continuum  $\psi$  coupled to a linear combination  $\alpha\psi_1 + \beta\psi_2$  of the confinement states in Eq. (3), and with a completely decoupled system for the orthogonal linear combination  $\beta\psi_1 - \alpha\psi_2$  in Eq. (4). Since, moreover,  $H_1$  and  $H_2$  are supposed to describe confinement, Eq. (4) has only bound-state solutions, all embedded in the meson-meson continuum.

### 3 The neutral kaon system

A typical example of the above-described phenomenon is the two-pion decay mode of the neutral kaon system. Both  $d\bar{s}$  and  $s\bar{d}$  couple weakly to  $\pi\pi$  via the process depicted in Fig. 1.

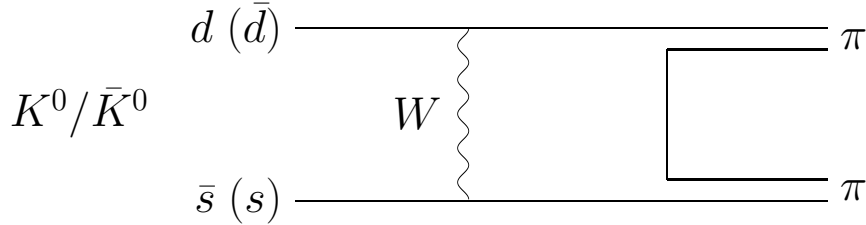


Figure 1:  $W$  exchange takes care of the flavour transitions triggering the strong process of quark-pair creation in weak  $K^0/\bar{K}^0$  two-pion decay.

Because of particle-antiparticle symmetry, we may assume  $\alpha = \beta = 1/\sqrt{2}$ . The  $CP = -1$  combination  $(d\bar{s} - s\bar{d})/\sqrt{2}$  completely decouples and turns into a bound state embedded in the  $\pi\pi$  continuum. This combination thus represents the  $K_L$  meson, which, since  $CP$  violation is not contemplated in our model, has no coupling to the two-pion continuum. However, the  $CP = +1$  combination  $(d\bar{s} + s\bar{d})/\sqrt{2}$  exists as a, actually extremely narrow, resonance in  $S$ -wave  $\pi\pi$  scattering, hence describing the  $K_S$  meson.

We assume here that the decay process depicted in Fig. 1 is dominated by the strong OZI-allowed  $^3P_0$  quark-pair-creation mechanism, whereas  $W$  exchange merely functions as a trigger to

this process, which basically only determines the decay probability. Hence, besides the smallness of the parity-violating  $K_S \rightarrow \pi\pi$  coupling constant, the transition potential describes here the coupling of a  $u\bar{u}$  state with  $J^{PC} = 0^{++}$ , i.e.,  $\sigma$ -meson quantum numbers to two pions, similar to our unitarised description of scalar mesons studied in Refs. [12, 13] (see also Ref. [14]). In the delta-shell approximation for the transition potential in the case of the scalar  $K_0^*(800)$  and  $a_0(980)$  resonances [12, 13], we obtained for the delta-shell radius  $a$  a value of about  $a = 3.2 \text{ GeV}^{-1}$ . We shall hold on to this value in the following.

A general solution of Eq. (3) for the  $S$ -wave scattering phase shift  $\cotg(\delta(s))$ , as a function of the total invariant two-pion mass  $\sqrt{s}$ , is in this approximation and for small coupling given by

$$\cotg(\delta(s)) \approx \frac{\left[ E_0 + R(s) |\mathcal{F}_0^{ds}|^2 \right] - \sqrt{s}}{I(s) |\mathcal{F}_0|^2} , \quad (5)$$

where  $E_0$  represents the ground-state energy of the  $d\bar{s}$  ( $s\bar{d}$ ) when uncoupled, hence the mass of the  $K_L$  meson. The remaining factors  $R(s)$ ,  $I(s)$ , and  $\mathcal{F}_0$  are well explained in Ref. [15]. From expression (5) it is easy to perturbatively extract the real and imaginary part of the resonance pole position in the complex-energy plane, i.e.,

$$E_{\text{pole}} \approx E_0 + \Delta E , \quad \text{with} \quad \Re(\Delta E) = R(s) |\mathcal{F}_0|^2 \quad \text{and} \quad \Im(\Delta E) = I(s) |\mathcal{F}_0|^2 . \quad (6)$$

The position of the  $K_S$  resonance pole with respect to the  $K_L$  mass is shown in Fig. 2. Since the coupling of the neutral kaons to the two-pion continuum is extremely small, the arrow pointing from  $\sqrt{s} = m_L$  to the  $K_S$  resonance pole position represents the pole trajectory for increasing intensity of the transition potential  $V_1$ , too.

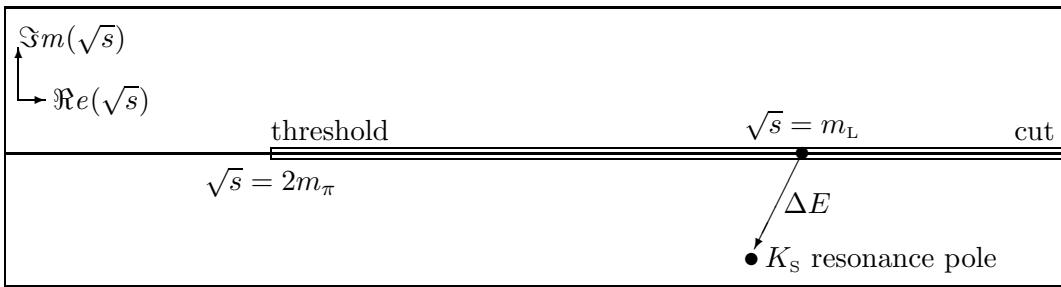


Figure 2:  $K_L$  bound-state pole embedded in the continuum, and  $K_S$  resonance pole in the second Riemann sheet.

For the ratio of the  $K_S$  decay width  $\Gamma_S$ , equalling twice the imaginary part (6) of the resonance pole position in the complex-energy plane, and the neutral-kaon mass difference, which equals

the real shift (6) of the pole with respect to  $E_0 = m_L$ , we read from formula (5) the result

$$\frac{\frac{1}{2}\Gamma_S}{m_S - m_L} \approx \frac{I(s)}{R(s)} \quad . \quad (7)$$

From Ref. [15] we moreover learn that, in the case of  $S$ -wave scattering, one has

$$\frac{I(s)}{R(s)} = \frac{j_0(ka)}{n_0(ka)} = -\text{tg}(ka) \quad . \quad (8)$$

As a consequence of Eqs. (5), (7), and (8), we obtain an extremely simple relation for the mass difference in the neutral kaon system, the width of the  $K_S$  meson, the two-pion momentum  $k$  and the strong-interaction radius  $a$ , reading

$$\frac{\frac{1}{2}\Gamma_S}{m_L - m_S} \approx \text{tg}(ka) \quad . \quad (9)$$

Substitution of  $k = 0.206 \text{ GeV}$  and  $a = 3.2 \text{ GeV}^{-1}$  gives us then the result

$$\frac{\frac{1}{2}\Gamma_S}{m_L - m_S} \approx 1.3 \quad (\text{Experiment: } 1.06 [8]) \quad . \quad (10)$$

Similar conclusions can be found in Refs. [16–20], where long-distance effects have been studied in more detail.

## 4 The $J^P = 1^+ \ c\bar{s}$ states

In the case of the  $J^P = 1^+ \ c\bar{s}$  states, we deal with two distinct systems,  $^3P_1$  and  $^1P_1$ , which, as far as confinement is concerned, are degenerate when ignoring possible spin-orbit effects. Both states couple strongly to  $D^*K$ , with threshold at about 2.501 GeV. In the case of the neutral kaon system, we could straightforwardly assume that the transition potentials  $V_1$  and  $V_2$  in Eq. (1) are equal, because of particle-antiparticle symmetry. But for the  $1^+ \ c\bar{s}$  systems we do not have such arguments. Nevertheless, if  $V_1$  and  $V_2$  are proportional, we still are in a situation comparable to the one discussed in the previous section, though now for strong interactions.

In Ref. [21] we showed how relative intensities, which can be defined according to

$$\frac{\int d^3r |V_2|^2}{\int d^3r |V_1|^2} \quad , \quad (11)$$

may be determined. For transitions to vector+pseudoscalar we find that the intensity for  $^3P_1$  is twice as large as for  $^1P_1$ . Consequently, by the use of Eqs. (4) and (3), we conclude that the  $J^P = 1^+ \ c\bar{s}$  bound state embedded in the  $D^*K$  continuum consists of a mixture of 33%  $^3P_1$  and 67%  $^1P_1$ , whereas its supposed resonance partner has more or less the opposite content, but additionally with some  $D^*K$  admixture.

In Sec. (3) we have used Eq. (3) for the description of  $\pi\pi$  scattering in the presence of the weak coupling to the neutral kaon system. Here, we assume that Eq. (3) is also suited to describe  $D^*K$  scattering in the presence of an infinity of  $c\bar{s}$  confinement states. In our unitarised model, this just implies substituting the effective nonstrange quark mass by the charmed quark mass, the pion masses by the  $D^*$  and  $K$  masses, and changing some of the quantum numbers. The scattering phase shift is given by an expression similar to the one shown in Eq. (5), but, since the interaction is not weak now, also higher radial excitations of the  $c\bar{s}$  confinement spectrum must be included. Thus, we use the general expression [12]

$$\cot g(\delta(s)) = \frac{n_0(pa)}{j_0(pa)} - \left[ 2\lambda^2 \mu p a j_0^2(pa) \sum_{n=0}^{\infty} \frac{|\mathcal{F}_n^{c\bar{s}}(a)|^2}{\sqrt{s} - E_n} \right]^{-1}. \quad (12)$$

Here, similarly to the procedure outlined in Ref. [12], we approximate the full sum over all  $c\bar{s}$  confinement states by the two nearest states, that is, the ground state at  $E_0$  and the first radial excitation at  $E_1$ , plus a rest term. The latter is scaled to 1 by absorbing its value into the coupling constant  $\lambda$ , yielding

$$\sum_{n=0}^{\infty} \frac{|\mathcal{F}_n^{c\bar{s}}(a)|^2}{\sqrt{s} - E_n} \longrightarrow \frac{0.5}{\sqrt{s} - E_0} + \frac{0.2}{\sqrt{s} - E_1} - 1 \text{ GeV}^2. \quad (13)$$

We determine the ground-state mass of the uncoupled system (4) from the model parameters given in Ref. [22], which gives  $E_0 = 2.545$  GeV. This also means that the bound state embedded in the  $D^*K$  continuum has exactly the mass  $E_0$ , only 9 MeV away from the experimental  $D_{s1}(2536)$  mass [8]. The first radial excitation lies  $2\omega = 380$  MeV higher.

In Fig. 3 we study how the position of the ground-state singularity in the scattering amplitude for Eq. (3) varies, as the intensity of the transition potential  $V_1$  is changed. In Nature one can only “measure” the pole position for one particular value of this intensity, given by strong interactions. Nevertheless, it is very illustrative to study alternative values. In particular, we notice that for larger intensities of the transition mechanism the pole comes out on the real  $E$  axis, below the  $D^*K$  threshold. Had we started from the perturbative formula (5), where  $R(s)$  and  $I(s)$  are proportional to  $\lambda^2$ , we would have started out as in Fig. 2, and never returned to the real  $E$  axis for increasing values of the transition intensity. The trajectory in Fig. 3 is highly nonperturbative, which can only be achieved when all orders [15] are accounted for. The masses obtained for the model’s values of  $\lambda$  are indicated by  $\bullet$  in Fig. 3. For the  $D_{sJ}^*(2463)$  we read from the figure  $m = 2.446$  GeV, so, after all, this state is not a resonance as one would naively (i.e., perturbatively) expect from the coupled set of equations (3), in agreement with experiment. As mentioned above, for the  $D_{s1}(2536)$  we obtain 2.545 GeV from pure confinement.

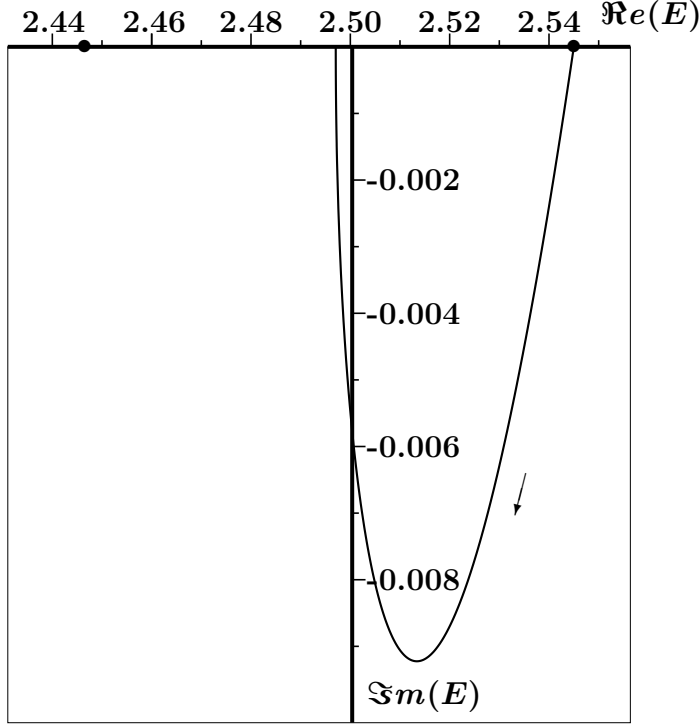


Figure 3: Trajectory of the ground-state pole in the  $D^*K$  scattering amplitude, as a function of the coupling constant  $\lambda$ , defined in Eq. (12), and which parametrises the intensity of the transitions between the pure  $c\bar{s}$  system and the  $D^*K$  continuum (see Eq. 3). The arrow indicates how the pole moves when  $\lambda$  is increased. For vanishing coupling, as well as for the confined system described by Eq. (4), the pole is on the real  $E$  axis. For large coupling we find the pole on the real  $E$  axis below threshold. Units are in GeV.

When the transition potentials  $V_1$  and  $V_2$  in Eq. (1) are not proportional, one has no simple diagonalisation, since commutators with the Hamiltonians will spoil the simplicity. Also, if  $H_1$  and  $H_2$  in Eq. (1) are not equal, diagonalisation will not lead to completely decoupled systems. However, from experiment we learn that the  $D^*K$  width of the  $D_{s1}(2536)$  is small (less than 2.3 MeV [8]), implying that the bulk of the interaction indeed stems from the unitarisation mechanism.

## 5 The $J^P = 1^+ c\bar{n}$ states

In order to describe the ground states of the  $J^P = 1^+ c\bar{n}$  spectrum, we use the same Eqs. (5) and (6) as in the previous case. Also here, we determine the ground-state mass of the uncoupled system (4) from the model parameters in Ref. [22], which now yields  $E_0 = 2.443$  GeV. Hence, the  $J^P = 1^+ c\bar{n}$  bound state embedded in the  $D^*\pi$  continuum comes out, in our model, at 2.443 GeV,

some 20 MeV above the experimental [8, 10]  $D_1(2420)$  mass. The first radial excitation lies, as before,  $2\omega = 380$  MeV higher.

The resulting cross section is given in Fig. 4. Our peak shows up somewhat above 2.3 GeV, whereas the width of our  $D_1(2420)$  is about 200 MeV. The corresponding experimental values are  $2400 \pm 30 \pm 20$  MeV [10] ( $2461^{+48}_{-42}$  MeV [11]), and  $380 \pm 100 \pm 100$  MeV [10] ( $290^{+110}_{-90}$  MeV [11]), respectively. In Fig. 4 we can further observe that the first radial excitation of the system

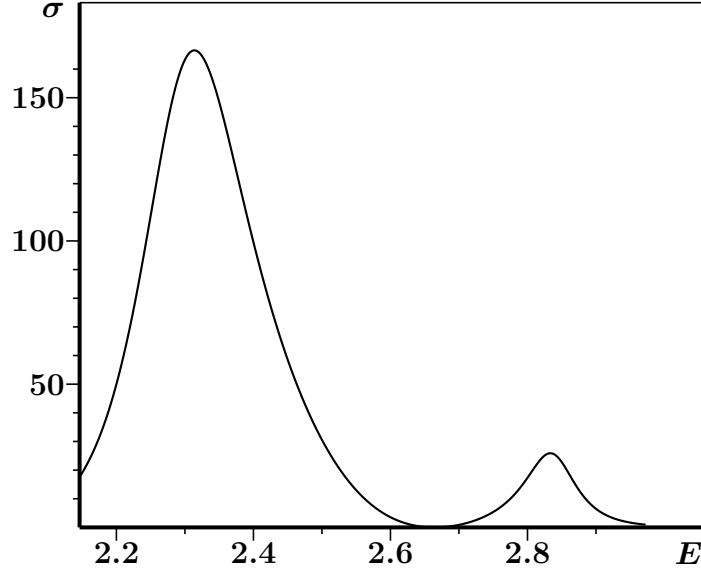


Figure 4: Model result for the cross section in units of  $\text{GeV}^{-2}$  for elastic  $S$ -wave  $D^*\pi$  scattering, as a function of the total invariant mass  $E$  in units of GeV.

of equations (3), for  $J^P = 1^+ c\bar{n}$ , comes out more than 500 MeV higher than the ground-state resonance. Nevertheless, in expression (6) we always used  $E_1 - E_0 = 380$  MeV [22]. Such a highly non-perturbative behaviour is inherent in the unitarisation procedure leading to formula (5).

The bound state  $D_1(2420)$  embedded in the  $D^*\pi$  continuum has zero width in our model, and so is invisible in the cross section of Fig. 4. On the other hand, experiment finds  $18.9^{+4.6}_{-3.5}$  MeV [8] and  $26.7 \pm 3.1 \pm 2.2$  [10] MeV for the full width, which is nonetheless very small as compared to the available phase space. Consequently, also in this case our assumption in Eq. (2) appears to be reasonable.

The relative intensities  $\alpha$  and  $\beta$  in Eq. (2) are the same as in the  $c\bar{s}$  case. Hence, the relative content of the  $D_1(2420)$  is again 33%  $^3P_1$  and 67%  $^1P_1$ . The  $D_1(2400)$  roughly has the opposite mixture, plus a  $D^*\pi$  component.

In Fig. 5 we show how the scattering pole moves in the complex-energy plane when  $\lambda$  is varied, which is the pole associated with the cross section of Fig. 4.



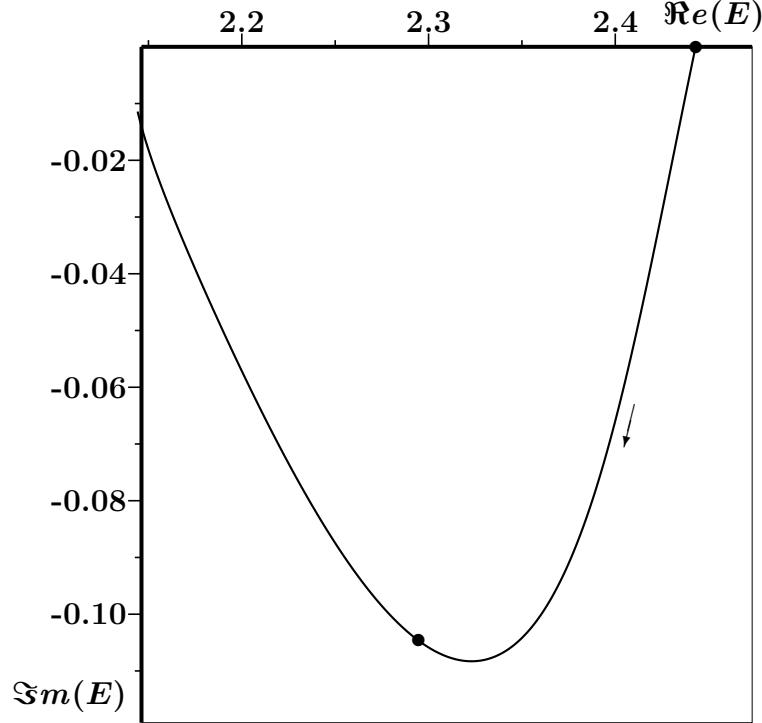


Figure 5: Trajectory of the ground-state pole in the  $D^*\pi$  scattering amplitude, as a function of the coupling constant  $\lambda$ . The arrow indicates how the pole moves when  $\lambda$  is increased. For vanishing coupling, as well as for the confined system described by Eq. (4), here representing the  $D_1(2420)$ , the pole is on the real  $E$  axis. The pole position for Eq. (3), which describes the  $D_1(2400)$ , is indicated by  $\bullet$  for the physical value of  $\lambda$ . Units are in GeV.

## 6 Summary and conclusions

In the present paper, we have studied examples of mesonic systems that generate bound or quasi-bound states in the continuum, within an unitarised quark-meson model. In the neutral-kaon system, our approach provides a simple explanation for the widths and the mass difference of the  $K_L$  and  $K_S$ , which is also in agreement with the conclusions of more sophisticated methods. Application to the  $J^P = 1^+ c\bar{s}$  and  $c\bar{n}$  axial-vector charmed mesons accomplishes a simultaneous description of the established narrow  $D_{s1}(2536)$  and  $D_1(2420)$  states, as well as the recently observed very narrow  $D_{sJ}^*(2463)$ , assuming it indeed is a  $1^+$  state, and broad  $D_1(2400)$ , which is rather problematic in standard quark models.

We predict that the continuum bound states  $D_1(2420)$  and  $D_{s1}(2536)$  are mixtures of 33%  $^3P_1$  and 67%  $^1P_1 c\bar{n}$ , respectively  $c\bar{s}$ , which possibly can be measured by radiative transitions [23]. For their partners  $D_1(2400)$  and  $D_{sJ}^*(2463)$  we predict more or less the opposite content, but additionally with some  $D^*\pi$ , respectively  $D^*K$  admixture.

With this achievement, we once again demonstrate that unitarisation has to be incorporated in realistic quark models of mesons and baryons, as it constitutes the second most important interaction after confinement.

## Acknowledgements

This work was partly supported by the *Fundação para a Ciência e a Tecnologia* of the *Ministério da Ciência e do Ensino Superior* of Portugal, under contract number POCTI/FNU/49555/2002.

## References

- [1] J. von Neumann and E. Wigner, Phys. Z. **30**, 465 (1929).
- [2] Lorenz S. Cederbaum, Ronald S. Friedman, Victor M. Ryaboy and Nimrod Moiseyev, Phys. Rev. Lett. **90**, 013001 (2003).
- [3] D. L. Pursey and T. A. Weber, prepared for *12th Int. Workshop on High-Energy Physics and Quantum Field theory (QFTHEP 97), Samara, Russia, 4-10 Sep 1997*, published in *Samara 1997, QFTHEP'97*, pp. 435-438.
- [4] H. C. Rosu and J. Socorro, Nuovo Cim. B **113**, 677 (1998) [arXiv:gr-qc/9610018].
- [5] A. Khelashvili and N. Kiknadze, J. Phys. A **29**, 3209 (1996) [arXiv:quant-ph/9511022].
- [6] J. Pappademos, U. Sukhatme and A. Pagnamenta, Phys. Rev. A **48**, 3525 (1993) [arXiv:hep-ph/9305336].
- [7] Eef van Beveren and George Rupp, Proc. Workshop *Recent Developments in Particle and Nuclear Physics, April 30, 2001, Coimbra (Portugal)*, ISBN 972-95630-3-9, pp. 1-16, [arXiv:hep-ph/0201006].
- [8] K. Hagiwara *et al.* [Particle Data Group Collaboration], Phys. Rev. D **66**, 010001 (2002).
- [9] D. Besson [CLEO Collaboration], arXiv:hep-ex/0305100.  
D. Besson *et al.* [CLEO Collaboration], to appear in Proc. *8th Conference on the Intersections of Particle and Nuclear Physics (CIPANP 2003), New York, 19-24 May 2003*, arXiv:hep-ex/0305017.
- [10] K. Abe *et al.* [BELLE Collaboration], BELLE-CONF-0235, contr. to *31st Int. Conf. on High Energy Physics (ICHEP 2002), Amsterdam, The Netherlands, 24-31 Jul 2002*.

- [11] S. Anderson *et al.* [CLEO Collaboration], Conference report CLEO-CONF-99-6, (1999).
- [12] Eef van Beveren and George Rupp, Eur. Phys. J. C **22**, 493 (2001) [arXiv:hep-ex/0106077].
- [13] Eef van Beveren and George Rupp, AIP Conf. Proc. **619**, 209 (2002) [arXiv:hep-ph/0110156].
- [14] M. D. Scadron, Mod. Phys. Lett. A **14**, 1273 (1999) [arXiv:hep-ph/9910244].
- [15] E. van Beveren and G. Rupp, Int. J. Theor. Phys. Group Theor. Nonlin. Opt., in press (2003) arXiv:hep-ph/0304105.
- [16] G. E. Brown, J. W. Durso, M. B. Johnson and J. Speth, Phys. Lett. B **238**, 20 (1990).
- [17] I. I. Bigi and A. I. Sanda, Phys. Lett. B **148**, 205 (1984).
- [18] P. Cea and G. Nardulli, Phys. Lett. B **152**, 251 (1985).
- [19] John F. Donoghue, Eugene Golowich and Barry R. Holstein, Phys. Lett. B **135**, 481 (1984).
- [20] J. Lowe and M. D. Scadron, arXiv:hep-ph/0208118.
- [21] Eef van Beveren and George Rupp, Phys. Lett. B **454**, 165 (1999) [arXiv:hep-ph/9902301].
- [22] E. van Beveren, G. Rupp, T. A. Rijken, and C. Dullemond, Phys. Rev. D **27**, 1527 (1983).
- [23] Stephen Godfrey, arXiv:hep-ph/0305122.